PROTECTING WELLHEAD QUALITY AND QUANTITY IN A CONTAMINATED AQUIFER

J. F. Sykes, Department of Civil Engineering, University of Waterloo, Waterloo, Ontario, Canada
S. D. Normani, Department of Civil Engineering, University of Waterloo, Waterloo, Ontario, Canada
M. I. Jyrkama, Department of Civil Engineering, University of Waterloo, Waterloo, Ontario, Canada

ABSTRACT
The protection of water quality and quantity at the Parkway Wellfield in Toms River, New Jersey requires careful management of pumping rates at the field's seven wells. To support this management, a detailed, three-dimensional, transient, highly calibrated groundwater model has been developed for the Cohansey aquifer. Well pumping rates as well as groundwater recharge have changed seasonally and yearly over the 32 year period since contaminants were illegally dumped at the Reich Farm Superfund site, north of the wellfield. The evolution of the wellfield combined with the spatially and temporally variable recharge in the Cohansey aquifer results in the fact that traditional steady-state capture zones may not permit the optimal management of the water quantity and quality at the Parkway wells. Rather, fully transient capture zones and analyses are required for wellhead management. The adjoint method applied to the contaminant transport equation is also used to define capture zones that include the effect of dispersion. Further, it is shown that while capture zones defined by average water particle paths can be used to manage water quality, other techniques such as the First-Order Reliability Method (FORM) combined with the adjoint sensitivity method provide the necessary input for the management of water quantity.

RÉSUMÉ
La protection de la qualité de l'eau et sa quantité au champs de puits de Parkway à Toms River, New Jersey, exige la gestion active des taux de pompage pour leurs sept puits. Pour aider à la gestion de la ressource, un modèle détaillé, fortement calibré, tridimensionnel, et variable en temps a été développé pour l'aquifère Cohansey. Au cours d'une période de 32 ans depuis que des contaminants ont été illégalement déchargés sur la site Superfund de la ferme Reich au nord du champs de puits, les taux de pompage ainsi que les taux d'alimentation des eaux souterraines ont changé annuellement avec des variations saisonnières. L'évolution du champs de puits ainsi que la variation spatialle et temporelle de l'alimentation de l'aquifère Cohansey signifie que les méthodes traditionelles pour identifier les zones de capture en état stationnaire ne permettront pas la gestion optimale de la qualité et quantité de l'eau des puits de Parkway. Plutôt, la modélisation et l'analyse des zones de capture en temps sont nécessaires pour la gestion des têtes de puits. La méthode d'adjoint (adjoint method) appliquée à l'équation de transport de contaminants est aussi employée pour définir les zones de capture qui incluent l'effet de la dispersion. De plus, tandis que des zones de capture définies par les chemins moyens des particules d'eau peuvent être employées pour gérer la qualité de l'eau, d'autres techniques telles que la méthode de fiabilité du premier ordre combinée avec la méthode d'adjoint fournissent les données nécessaires pour la gestion de sa quantité.

1. INTRODUCTION

A statistically significant childhood cancer cluster has been identified in Toms River, New Jersey (see Figure 1). A case-control epidemiological study into the cause of the cancer included an investigation of the quality of the groundwater used to supply the municipal water distribution system. Historically, groundwater for the water distribution system was supplied by numerous wells including five wells that are part of the Parkway Wellfield. The Parkway wells are approximately 1600 m down gradient from the Reich Farm Superfund site. The contaminants that migrated from the site, through the Cohansey aquifer, and entered one or more of the Parkway wells included trichloroethylene (TCE), perchloroethylene (PCE) and a styrene-acrylonitrile (SAN) trimer. An additional well was installed at the wellfield to further control the contaminant plume entering some Parkway wells and to maximize the quantity of water pumped from the aquifer. The water from three wells is treated using an air stripper and carbon adsorption columns, and then discharged to the ground surface in an area southwest of the wellfield. Water from the remaining Parkway wells is used to supply the municipal water distribution system.

2. SITE DESCRIPTION

2.1 Spatial Domain

The modelling domain is bounded on the west by the Toms River, on the south by the Toms River estuary, on the east by Barnegat Bay and along the north by a surface water divide and assumed groundwater divide. The top of the model is defined by a Digital Elevation Model (DEM) obtained from the New Jersey Geological Survey, while the bottom of the domain represents the interface between the bottom of the Cohansey-Kirkwood aquifer and the top of a basal clay layer as defined by Zapecza

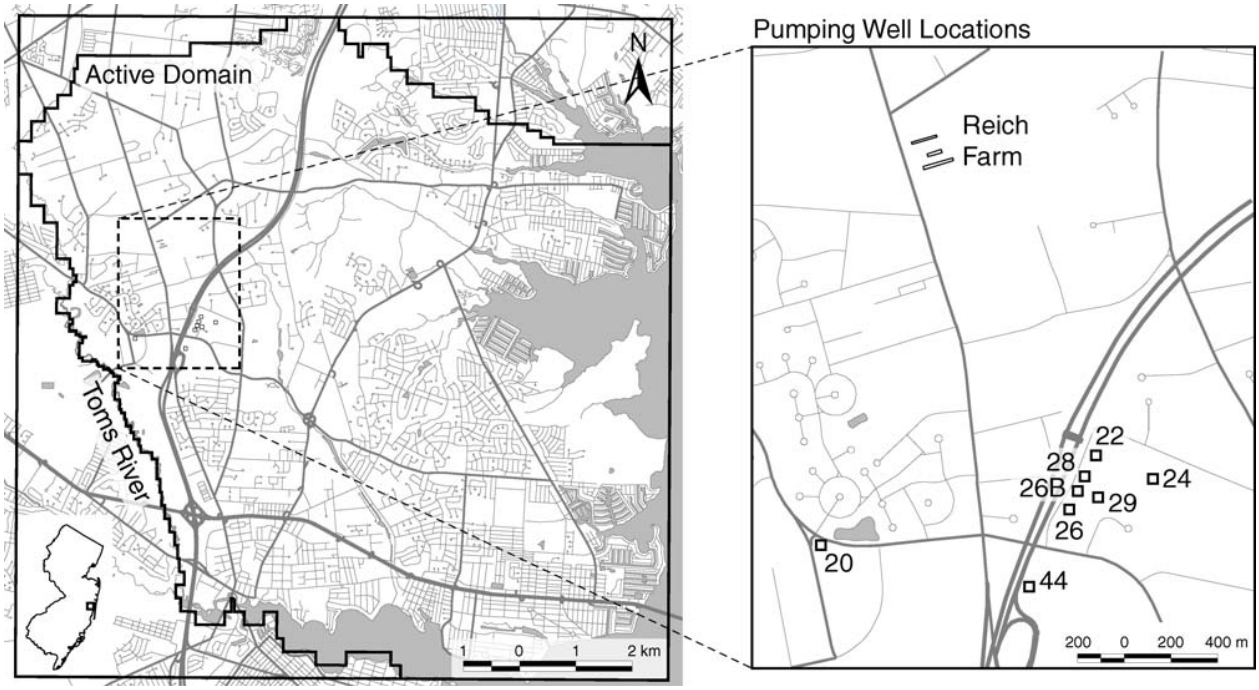

Figure 1. Site map showing location of Toms River in New Jersey, the modelling domain, and the location of the Reich Farm Superfund site and the various municipal pumping wells

(1989). The interface between the Cohansey and Kirkwood aquifers is interpolated from driller's logs that entered the Kirkwood formation, where the Kirkwood formation is identified by fine gray sands and silts, and gray clays. The locations of these wells were determined from a combination of information provided on the well records, well permits, tax maps, a tax database, property locations by street address and lot/block, as well as the 1995/97 aerial digital orthophotography from the New Jersey Department of Environmental Protection (NJDEP). The use of ArcView GIS was integral to the management of the data and determination of well coordinates. The MODFLOW model is comprised of 200 columns, 208 rows, and 4 layers; of which the top three layers represent the higher conductivity Cohansey aquifer, while the bottom layer represents the lower conductivity Kirkwood aquifer.

2.2 Boundary Conditions

Boundary conditions for the top surface of the model domain were represented by prescribed Type I Dirichlet boundary conditions (general head boundary (GHB) condition as implemented in MODFLOW), leakance from surface water bodies such as rivers, lakes, and ponds, and recharge from precipitation. Figure 2 depicts the various boundary conditions that were assigned to the layer 1 grid blocks.

The Toms River estuary and Barnegat Bay were represented using a general head boundary condition (see Figure 2). Head elevations for these grid blocks were set to zero feet AMSL, and a high conductance was selected for these blocks. The Rivers and Surface Water categories as shown in Figure 2 are represented in the model using the MODFLOW river package. The surface water bodies in the model were described using river width and length in a grid block, conductance, stage elevation, and water depth. Stage elevations of rivers and

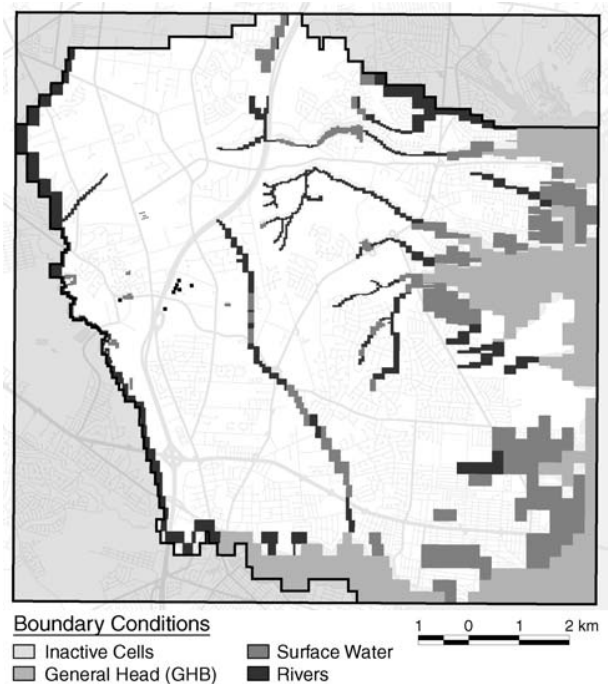

Figure 2. Boundary conditions applied to layer 1 of the groundwater flow model

lakes or ponds were estimated from the USGS 7.5 minute quadrangle maps as the DEM was not sufficiently accurate to determine the elevation of surface water bodies. GIS layers for rivers, ponds and lakes were obtained from the NJDEP. Some of these GIS layers were corrected to reflect the actual locations of water features as shown in the USGS quadrangle maps for the area. ArcView GIS was used to facilitate the calculation of the grid block properties and to create some MODFLOW input files. Stage elevations, surface water body areas, and conductances were assumed to be temporally invariant.

Recharge for the domain varies both spatially and temporally. A combination of land use, soil maps, daily precipitation and temperature over a 30+ year time span, and the HELP3 (Hydrologic Evaluation of Landfill Performance) model were used in a database / ArcView framework to develop monthly recharge values (that vary in time and in space) for each recharge grid block. This approach is documented in Jyrkama (2002). Figure 3 shows the average monthly recharge for the ten year period from 1981 to 1990.

2.3 Pumping Wells

Eight municipal pumping wells that pump water from the Cohansey aquifer are shown in Figure 1. The Parkway Wellfield is comprised of Wells 22, 24, 26, 26B, 28, and 29. Pumping volumes for the eight wells from 1981 to 2001 are shown in Figure 4.

The eight wells shown on Figure 1 have not operated in a continuous manner as demonstrated in Figure 4. Some wells such as 26B and 44 are relatively new, while Well 20 has ceased operation as of mid-1997. The remaining Parkway wells have operated at variable rates depending on the consumer demand for water, which varies from season to season. Wells 22 and 28 have steadily increased their pumping rates over the 20 years, while Well 26's pumping rates decreased during the 1990's. The well was redeveloped, thereby increasing its capacity.

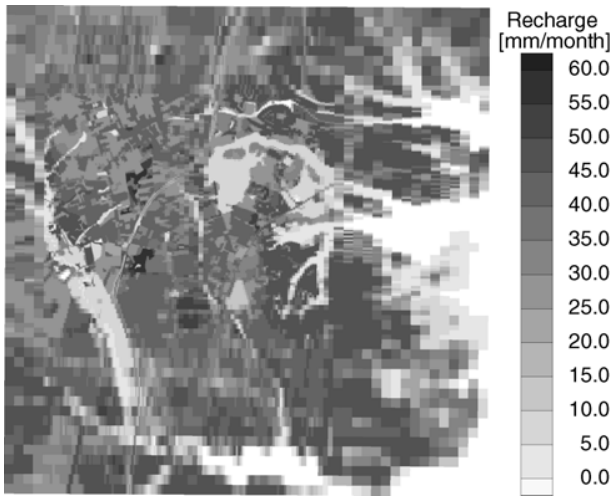

Figure 3. Ten year temporally averaged, spatially variable recharge for 1981 through 1990

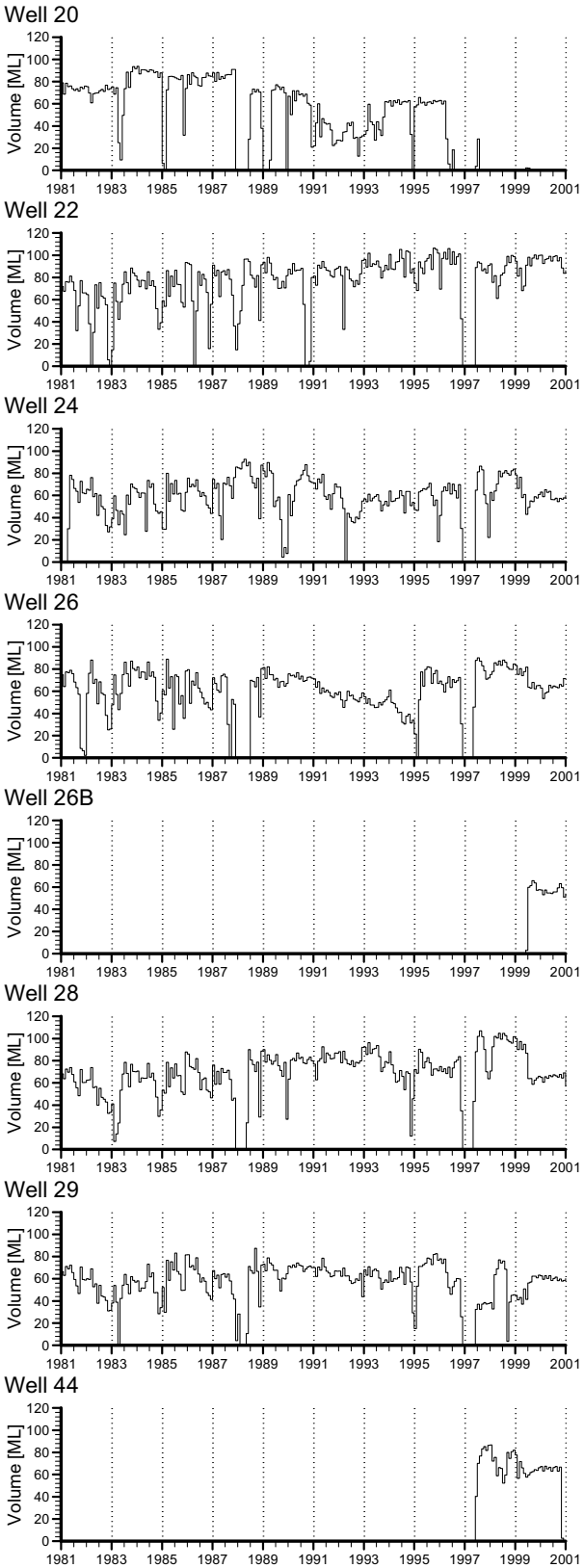

Figure 4. Monthly pumping volumes for various wells from 1981 to 2001

3. WATER QUALITY

3.1 Capture Zones

In order to better protect groundwater resources, capture zone analysis is typically performed using steady state reverse particle tracking. Although this practice is common, it does not account for the transient behaviour of wells, the evolution of groundwater flow systems, or the effects of seasonally and/or annually varying rainfall and temperature. The temporally averaged recharge and pumping rates from 1981 to 1990 were used to model the steady state capture zones for the 1991 to 2001 time period. Transient capture zones were also modelled using the recorded precipitation, temperature, and well pumping rates. The modelling illustrates the differences between the steady state and the transient analyses.

3.1.1 Steady State Capture Zones

Well pumping rates for the January 1981 to December 1990 period were averaged to obtain the steady state pumping rates for the steady state capture zone analysis. Monthly spatially variable recharge was averaged over the same ten year period to yield the temporally averaged, spatially variable recharge shown in Figure 3. Reverse particle tracking was performed using MODPATH to yield Figure 5.

Figure 5. Ten year steady state capture zones for wells

3.1.2 Transient Capture Zones

The transient capture zone analysis was performed by generating a grid of particles (151 rows by 131 columns) on a 30.48 m (100 ft) grid at the beginning of each month, from October 1971 to December 2000 for a total of 6,830,589 particles (some particles were not within the active modelling domain and are excluded). Each particle was tracked to determine its destination, whether to a well or otherwise. Figure 6 demonstrates all particles released in January 1991 that entered one of the eight wells within 10 years. As can be seen, the capture zones are slightly different as compared to Figure 5. Some notable differences can be seen with Well 20, as it was shutdown a few years into the future, as viewed from the perspective of when these particles were released. The capture zones for Well 22 and Well 24 are relatively stable and can be traced back to the fact that the pumping rates for these wells are mostly maintained at steady state values during the 1990's. Other wells show a marked difference, namely Wells 26B and 44 which did not exist in 1991 and whose presence was not anticipated. This has the effect of changing the capture zones of neighbouring wells 26, 28, and 29. Some particles in the vicinity of Reich Farm can be seen to enter Well 26B within 10 years, although Well 26B does not yet exist in 1991. Variations in the pumping rates at the various wells is demonstrated in the jaggedness of the capture zones. The capture zone for Well 22 contains particles that will be captured by Well 28, since Well 22 will be shutdown at some point in the future (late 1996). The same can be said of Well 28 particles dispersed within the Well 29 or Well 26 capture zones.

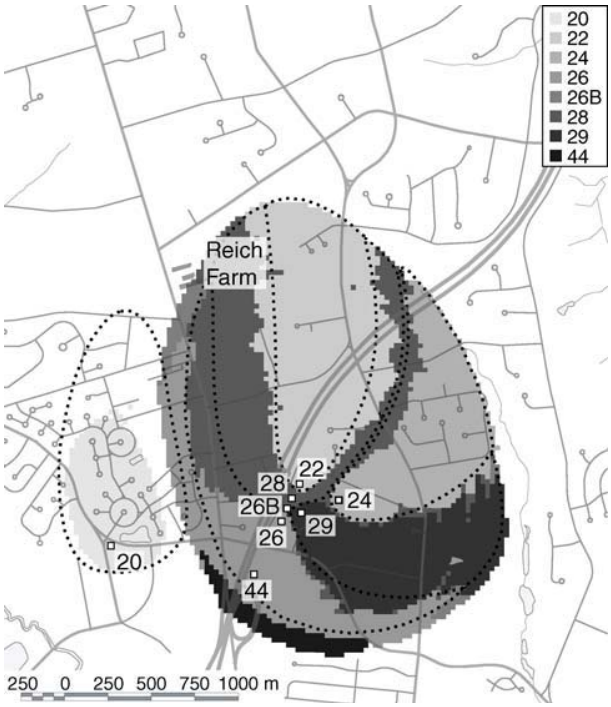

Figure 6. Average water particles released in January 1991 that arrived in a well within ten years

Given that a particle released at a particular location may enter different wells depending on when it was released, particle likelihood maps have been generated to demonstrate the likelihood that an average water particle entered a particular well. The likelihood is calculated as

the number of average water particles entering a given well divided by the number of average water particles that entered any well. This approach would exclude particles that have not yet reached a destination; either a well, or sink such as a river or lake. Average water particles move with the interstitial groundwater flow velocity and do not represent the migration of contaminants, many of which are affected by adsorption, diffusion, and dispersion mechanisms.

Figure 7 represents the likelihood of an average water particle entering Well 20 from October 1971 to December 2000. In the vicinity of Reich Farm, the likelihood increases in a westerly direction because Well 20 was in operation several years prior to the development of the Parkway Wellfield. As the groundwater flow system evolved due to pumping at the Parkway Wellfield, average water particles that would have originally migrated to Well 20, then migrate to Wells 26, 26B, or 28 (see Figures 8, 9, and 10).

The likelihood map for Well 26 (see Figure 8) is relatively stable and conforms quite well to the capture zones in Figures 5 and 6. Well 26B in Figure 9 shows a low likelihood of average water particle capture because Well 26B was placed into operation in 1999. The likelihood is greatest at the ends of the capture zones, as this allows more travel time for the average water particles and they are more likely to be captured by Well 26B as it develops its capture zone into the future. Figure 10 illustrates the likelihood of capture for Well 28. As can be seen, Well 28 will, on occasion, capture average water particles that originate in Well 22's capture zone. A few instances exist a whereby Well 22 was turned off, while Well 28 continued to pump. Average water particles that had migrated toward Well 22 while it was pumping, which were close to being captured, were not as the well was turned off. Since Well 28 was nearby and pumping, these average water particles were captured by Well 28.

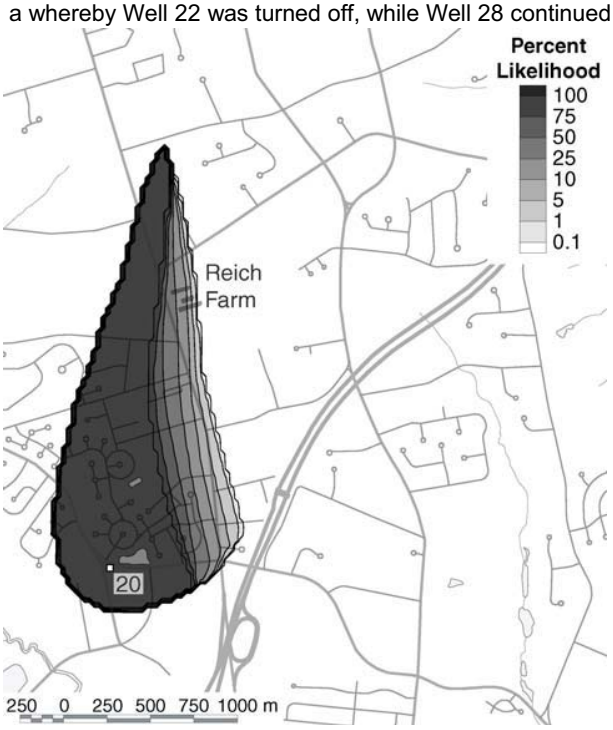

Figure 7. Likelihood of an average water particle entering Well 20 from Oct. 1971 to Dec. 2000

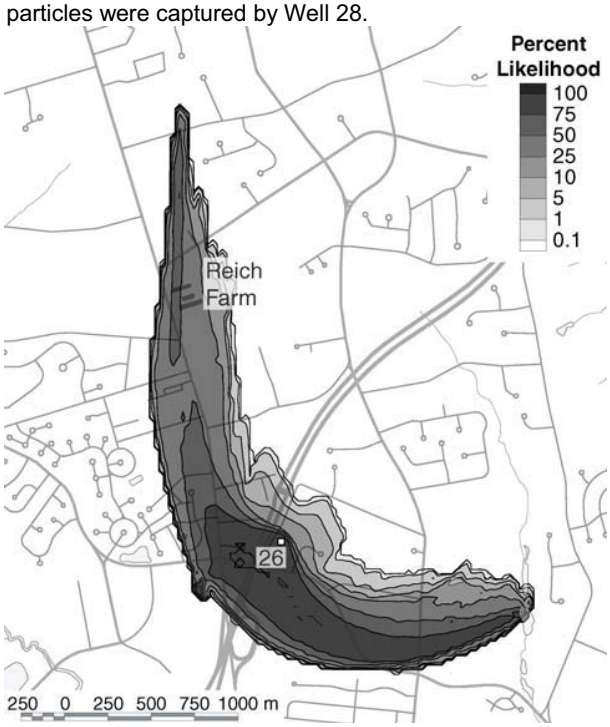

Figure 8. Likelihood of an average water particle entering Well 26 from Oct. 1971 to Dec. 2000

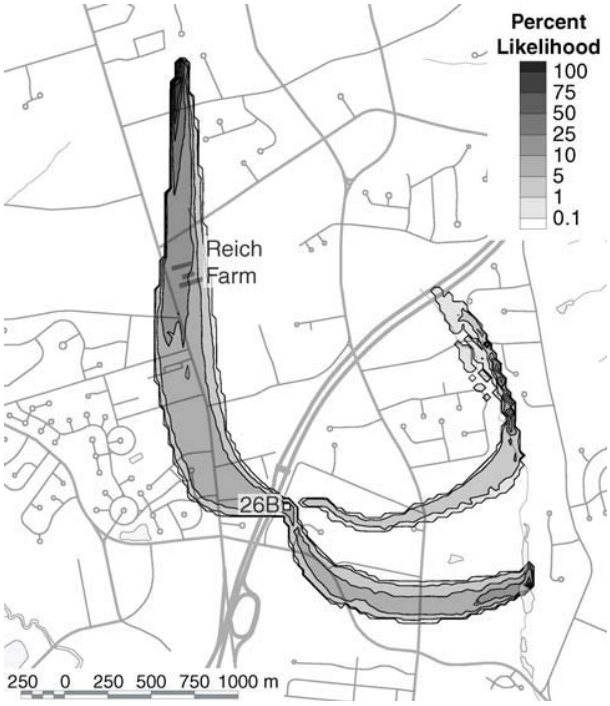

Figure 9. Likelihood of an average water particle entering Well 26B from Oct. 1971 to Dec. 2000

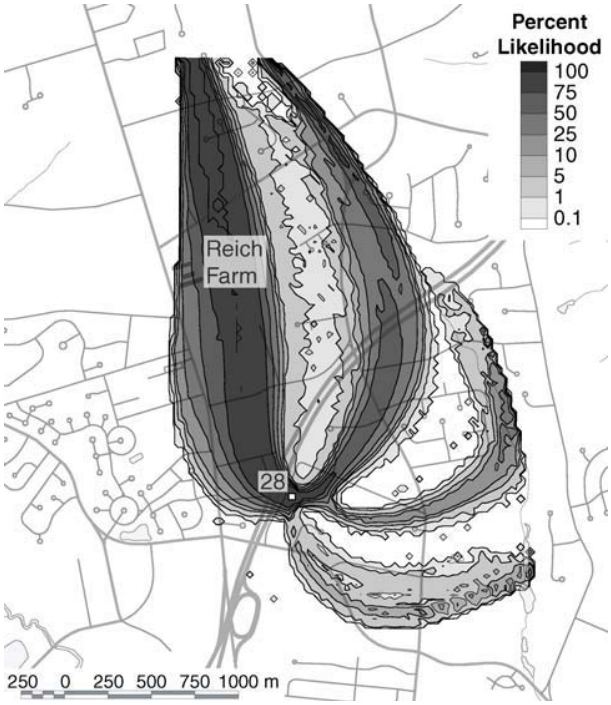

Figure 10. Likelihood of an average water particle entering Well 28 between Oct. 1971 and Dec. 2000

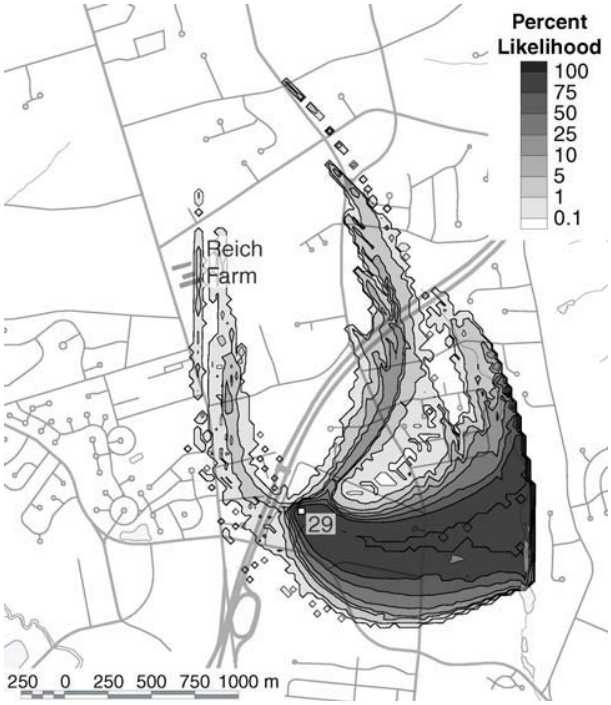

Figure 11. Likelihood of an average water particle entering Well 29 between Oct. 1971 and Dec. 2000

Figures 11 and 12 illustrate that particles which would mostly be captured by Wells 26, 26B, or 28, can be captured, under some circumstances, by Wells 29 and 44. An analysis of when these particles arrived at Well 29 can

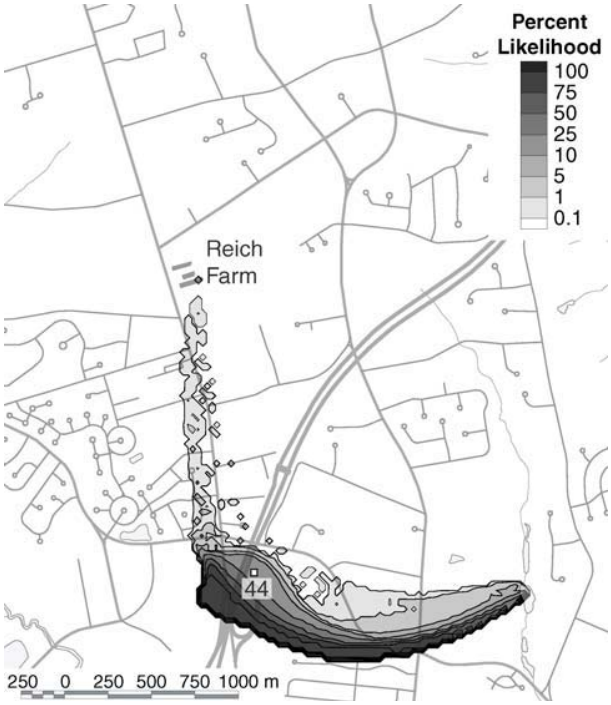

Figure 12. Likelihood of an average water particle entering Well 44 between Oct. 1971 and Dec. 2000

be seen in Figure 13. The majority of these particles arrived pre-1985 as compared to post-1985. Approximately 0.56% of average water particles originated northwest of Well 29. For Well 44 (see Figure 14), approximately 0.82% of average water particles originated north of Well 44 and entered between July 1998 and April 2000.

3.1.3 Backward Advective Dispersive Transport

The forward advective dispersive solute transport equation is defined as:

$$\theta \frac{\partial C}{\partial t} = \frac{\partial}{\partial x_i}\left(D_{ij}\frac{\partial C}{\partial x_j}\right) - q_i \frac{\partial C}{\partial x_i} \qquad [1]$$

where θ is the porosity, D_{ij} is the dispersivity tensor, q_i is the darcy flux, t is time and C is the concentration. The adjoint of the advective dispersive solute transport equation is:

$$-\theta \frac{\partial \beta^*}{\partial t} = \frac{\partial}{\partial x_j}\left(D_{ji}\frac{\partial \beta^*}{\partial x_i}\right) + q_i \frac{\partial \beta^*}{\partial x_i} + \frac{\partial f(\alpha, C)}{\partial C} \qquad [2]$$

where β^* is the adjoint state variable, or importance function, and α is any model input variable. Equation 2 is solved backward in time from a prescribed final state. To investigate the sensitivity to the concentration in a pumping well,

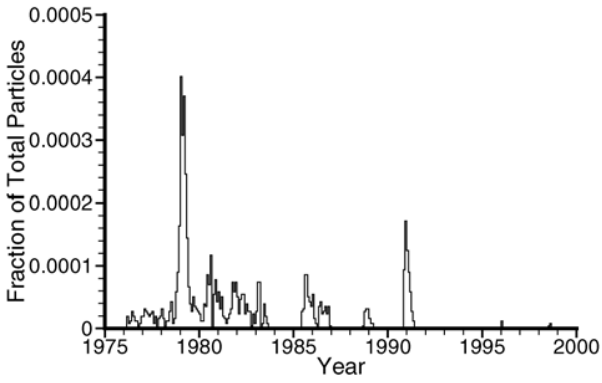

Figure 13. Fraction of average water particles that arrive at Well 29 in each month from the northwest

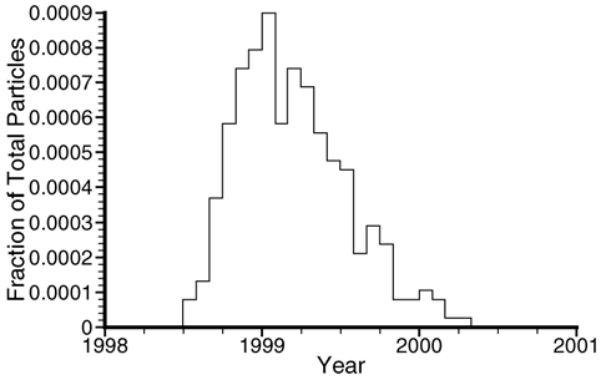

Figure 14. Fraction of average water particles that arrive at Well 44 in each month from the northwest

$$\frac{\partial f(\alpha, C)}{\partial C} = \frac{\partial}{\partial C_w}\{Q_i C_i\} = \begin{cases} 0 \text{ for } i \neq w \\ Q_i \text{ for } i = w \end{cases} \quad [3]$$

In other words, the concentration applied to the backwards problem is unity at the specified pumping well, and zero elsewhere. The adjoint of the forward advective dispersive equation represents the backward advective dispersive equation. A benefit of using an advective dispersive simulation is that dispersion and diffusion are accounted for, whereas average water particle tracking does not include these transport processes.

MT3DMS was used to perform the backward solute transport simulations. The input data files for MT3DMS were processed to reverse the time step order, as well as reversing the fluxes, velocities, and storage terms calculated from the forward transient groundwater flow simulations. One simulation was performed for each well with a unit concentration applied to the appropriate well. The ten year results for several wells are described in the following paragraphs.

Figure 15 shows the importance function for Well 26. As in the comparison for Well 20, we can see that dispersion tends to lengthen the zone of impact and make it wider. A small lobe can also be seen northeast of the well.

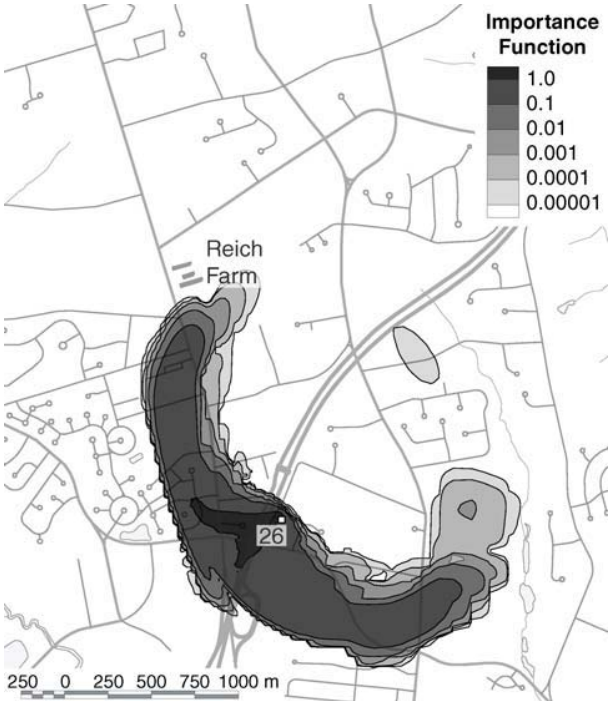

Figure 15. Importance function for Well 26 in January 1991

Similarly, Well 26B is shown in Figure 16; since Well 26B was installed in 1999, regions of greater importance are shown to be further away from the well. Figure 17 for Well 28 also demonstrates the effects of Well 22 being turned off as previously shown in Figure 10. Figure 18 for Well 29 shows that Well 29 obtains most of its water from the east although some comes from the west, and is different than the steady state capture zones shown in Figure 5.

4. WATER QUANTITY

Management of a well requires the consideration of both water quality and quantity aspects. While land use management within the well capture zone is an effective way of protecting the well from contamination, the head and hence, production at the well is not controlled only by the well capture zone, but by the wider aquifer system.

Groundwater flow is influenced both by the physical characteristics of the aquifer, as well as the recharge boundary condition. While recharge is affected by a multitude of factors, such as climatic conditions and the nature of the unsaturated zone, it is also influenced by land surface parameters such as land use and vegetation (Sharma, 1989). Therefore, any changes in land use will not only influence the groundwater flow system, i.e. heads at specific locations, through the recharge mechanism, but will also impact the extent and configuration of well capture zones.

In the present study, the highly variable recharge boundary condition for the groundwater model incorporated detailed information about the land use and land cover in the study area. The impact of the recharge

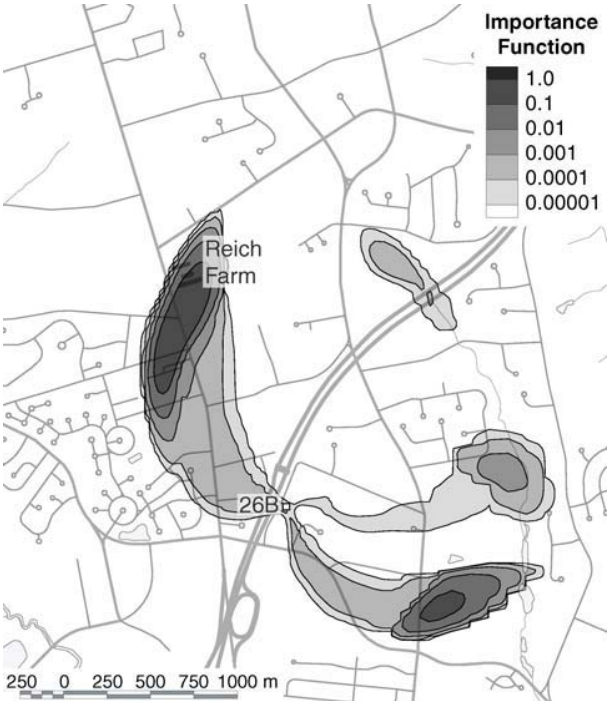

Figure 16. Importance function for Well 26B in January 1991

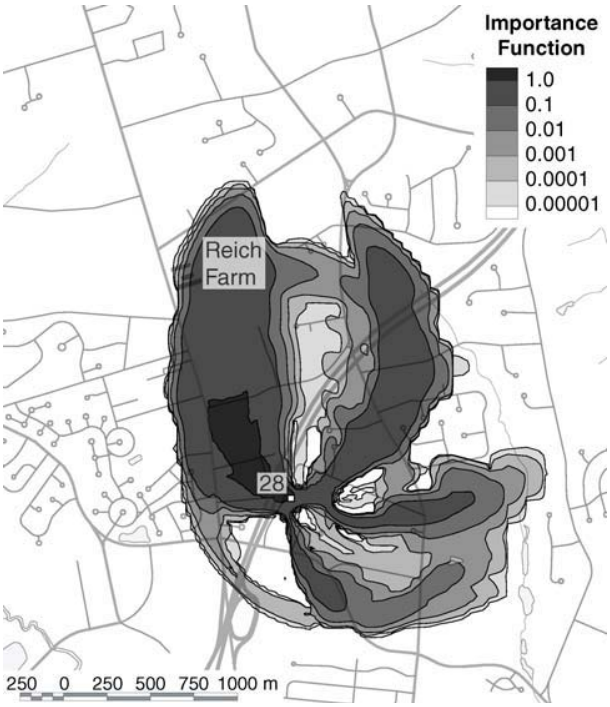

Figure 17. Importance function for Well 28 in January 1991

boundary condition, and hence land use, on the head or flow rate at a pumping well are therefore investigated by integrating the reliability analysis method with MODFLOW.

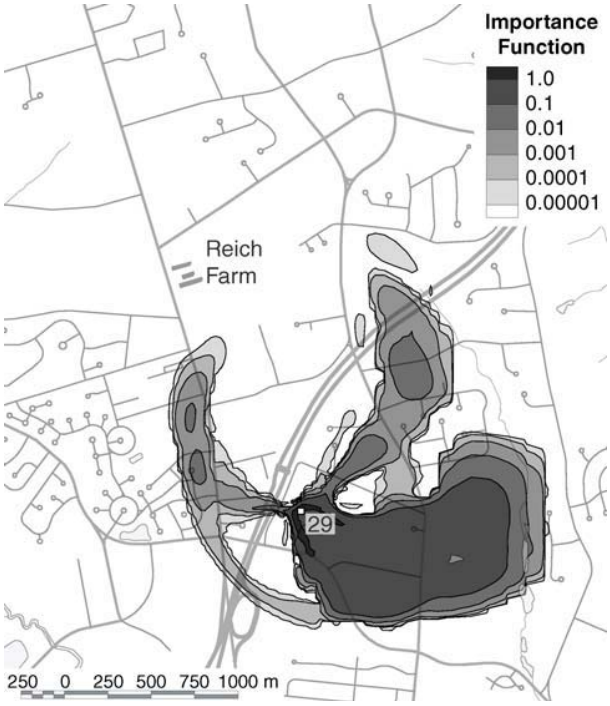

Figure 18. Importance function for Well 29 in January 1991

4.1 Reliability Analysis

Reliability analysis (e.g. the first- and second-order reliability methods FORM and SORM) are based on the formulation of failure criteria which is flexible and applicable to a wide spectrum of problems and events (e.g. Sitar, 1987 and Jang, 1994). The main advantage of the method over other approaches, besides high computational efficiency, is that it not only provides sensitivity information as an integral part of the solution, but it also determines the combination of model parameters that are most likely to result in the failure condition. This is very useful for studies with a large number of uncertain variables, such as grid based groundwater modelling investigations. The sensitivity information also identifies parameters that have the highest influence on the solution, which can be used to assess the impact of the recharge boundary condition on the groundwater flow system.

Consider the limit-state equation, or performance measure M as

$$M = g(\mathbf{X}) = w(\mathbf{u})\left[h_S(\mathbf{u}) - h_T\right] \quad [4]$$

where **X** denotes the uncertain boundary recharge fluxes, w(**u**) is an arbitrary weighting function denoting the location of importance, **u** is the location vector, h_S is the simulated head, and h_T is the specified target head. The limit-state equation is therefore solely a function of piezometric head and only indirectly related to recharge through the heads. To simplify the analysis, we select a

single location of interest coinciding with the location of a pumping well (i.e. Well 22) such that

$$w(\mathbf{u}) = \delta(\mathbf{u} - \mathbf{u}_{PW-22}) \quad [5]$$

where δ denotes the Dirac delta. The failure condition associated with the limit-state equation, therefore, indicates the probability that the head at Well 22 would fall below a certain specified level h_T, due to uncertainties in the estimated recharge distribution. Or in other words, the probability associated with exceeding a specified drawdown at the well.

The probability of failure is obtained by

$$P[g(\mathbf{X}) \le 0] = \int_{g(\mathbf{X})\le 0} f_x(\mathbf{x})dx \quad [6]$$

where $f_X(x)$ is the joint PDF of **X** integrated over the entire failure domain. The first-order approximation of the probability of failure is estimated as

$$P_f \approx \Phi(-\beta) \quad [7]$$

where Φ is the standard normal CDF and β is the reliability index.

The reliability index is defined as the closest distance from the origin to the failure surface in standard normal space, also known as the design point Y*, and is estimated according to the non-linear constrained optimization problem

$$\mathbf{Y}_{k+1} = \frac{1}{\left|\nabla G(\mathbf{Y}_k)\right|^2}\left[\nabla G(\mathbf{Y}_k)^T \cdot \mathbf{Y}_k - G(\mathbf{Y}_k)\right]\nabla G(\mathbf{Y}_k) \quad [8]$$

which can be solved using the efficient and robust HL-RF algorithm (Hasofer, 1974 and Rackwitz, 1978).

The sensitivity of β with respect to equally likely changes in the random variables is described by the unit gamma sensitivity vector as

$$\boldsymbol{\gamma} = \frac{(\nabla\beta)\mathbf{D}}{\left|(\nabla\beta)\mathbf{D}\right|} \quad [9]$$

where **D** is the diagonal matrix of standard deviations.

The evaluation of the gradient sensitivity vector $\nabla G(\mathbf{Y})$ in grid based numerical models can become very demanding computationally, due to the potentially large number of random variables resulting from model discretization. This challenge is overcome by implementing the adjoint method for flow in MODFLOW.

4.2 Adjoint Method

The equations used to solve the groundwater flow problem in MODFLOW are described in matrix form as

$$\mathbf{A}(\boldsymbol{\theta},\mathbf{h})\mathbf{h} = \mathbf{q}(\hat{\boldsymbol{\eta}}) \quad [10]$$

where A is the symmetric matrix of head coefficients, θ are system parameters, h are the head values, and q is the vector of constant terms, or RHS, which is a function of the model boundary conditions $\hat{\boldsymbol{\eta}}$ (McDonald, 1996). In this study, only the recharge rates are assumed to be random or uncertain, while all other model parameters are assumed to be constant (i.e. deterministic).

The solution of the first-order reliability problem requires the sensitivity of the limit-state equation with respect to the recharge boundary condition. The marginal sensitivity of the performance measure M with respect to the recharge rates X is

$$\frac{\partial M}{\partial \mathbf{X}^T} = \frac{\partial M(\mathbf{h})}{\partial \mathbf{h}^T}\frac{\partial \mathbf{h}}{\partial \mathbf{X}^T} \quad [11]$$

Expressing the flow problem in terms of head and recharge only, and differentiating with respect to X gives

$$\frac{\partial \mathbf{A}(\mathbf{h})}{\partial \mathbf{h}^T}\frac{\partial \mathbf{h}}{\partial \mathbf{X}^T}[\mathbf{I} * \mathbf{h}] + \mathbf{A}(\mathbf{h})\frac{\partial \mathbf{h}}{\partial \mathbf{X}^T} = \frac{\partial \mathbf{q}(\mathbf{X})}{\partial \mathbf{X}^T} \quad [12]$$

where **I** is the identity matrix and * denotes the Kronecker or outer product. Representing the state sensitivity $d\{h\} / d\{\mathbf{X}\}^T\}$ as $\boldsymbol{\psi}$, the adjoint equations of the partial differential equations are formulated by multiplying [12] by an arbitrary differentiable constant $\tilde{\boldsymbol{\psi}}$ and subtracting the result from [11] to give

$$\frac{\partial M}{\partial \mathbf{X}^T} = \left[\frac{\partial M(\mathbf{h})}{\partial \mathbf{h}^T}\right]\boldsymbol{\psi} + \tilde{\boldsymbol{\psi}}^T\left[\frac{\partial \mathbf{A}(\mathbf{h})}{\partial \mathbf{h}^T}\boldsymbol{\psi}[\mathbf{I} * \mathbf{h}]\right] + \tilde{\boldsymbol{\psi}}^T\mathbf{A}(\mathbf{h})\boldsymbol{\psi} - \tilde{\boldsymbol{\psi}}^T\frac{\partial \mathbf{q}(\mathbf{X})}{\partial \mathbf{X}^T} \quad [13]$$

Collecting terms,

$$\frac{\partial M}{\partial \mathbf{X}^T} = \left(\left[\frac{\partial M(\mathbf{h})}{\partial \mathbf{h}^T}\right] + \tilde{\boldsymbol{\psi}}^T\left[\frac{\partial \mathbf{A}(\mathbf{h})}{\partial \mathbf{h}^T}[\mathbf{I} * \mathbf{h}]\right] + \tilde{\boldsymbol{\psi}}^T\mathbf{A}(\mathbf{h})\right)\boldsymbol{\psi} - \tilde{\boldsymbol{\psi}}^T\frac{\partial \mathbf{q}(\mathbf{X})}{\partial \mathbf{X}^T} \quad [14]$$

Since $\tilde{\boldsymbol{\psi}}$ is arbitrary, we let

$$\left[\frac{\partial M(\mathbf{h})}{\partial \mathbf{h}^T}\right] + \tilde{\boldsymbol{\psi}}^T\left[\frac{\partial \mathbf{A}(\mathbf{h})}{\partial \mathbf{h}^T}[\mathbf{I} * \mathbf{h}]\right] + \tilde{\boldsymbol{\psi}}^T\mathbf{A}(\mathbf{h}) = 0 \quad [15]$$

Therefore,

$$\left[\mathbf{A}(\mathbf{h}) + \frac{\partial \mathbf{A}(\mathbf{h})}{\partial \mathbf{h}^T}[\mathbf{I} * \mathbf{h}]\right]^T\tilde{\boldsymbol{\psi}} = \frac{\partial \mathbf{M}(\mathbf{h})}{\partial \mathbf{h}^T} \quad [16]$$

where $\tilde{\boldsymbol{\psi}}$ represents the adjoint state or importance function (Sykes, 1985). As shown in [4], the performance function is formulated in terms of the piezometric head and the weighing function w(**u**). The load term on the right hand side of [16] therefore becomes

$$\frac{\partial \mathbf{M}(\mathbf{h})}{\partial \mathbf{h}^T} = w(\mathbf{u}) \quad [17]$$

As indicated by [5] the weighing function is equal to 1 at the pumping well, and zero elsewhere. The second term on the left hand side of [16] can be shown to have a negligible impact on the convergence of the reliability solution, and is therefore ignored. This simplifies [16] to

$$\mathbf{A}(\mathbf{h})^T \tilde{\boldsymbol{\psi}} = w(\mathbf{u}) \quad [18]$$

The importance function, therefore, represents the increase of head at all locations in the domain due to a unit volumetric influx of water at the well.

Because q is formulated in terms of recharge volume in MODFLOW, the marginal sensitivity of the performance measure with respect to the system parameters simplifies to

$$\frac{\partial M}{\partial \mathbf{X}^T} = \nabla g(\mathbf{X}) = -\tilde{\boldsymbol{\psi}}^T \Delta \mathbf{r} \Delta \mathbf{c} \quad [19]$$

where Δr and Δc denote the dimensions of the finite difference grid blocks in the row and column directions, respectively. The sensitivity of head at the well with respect to the recharge boundary condition $\nabla g(\mathbf{X})$ is therefore simply equal to the value of the importance function $\boldsymbol{\psi}$ in each grid block multiplied by the horizontal grid block area.

4.3 MODFLOW Implementation

Evaluation of the gradient sensitivity vector requires the solution of [10] which is termed the forward problem and is solved first for the coefficient matrix A and the head distribution h, while [18] is defined as the backward problem and is used to calculate the importance function $\boldsymbol{\psi}$ for a given performance function M. The backward problem can be readily solved using MODFLOW by: 1) running MODFLOW (forward problem) to obtain the A matrix, 2) setting the RHS vector equal to zero, except for the grid cell containing the pumping well, which is set to one, and 3) re-running MODFLOW using the new RHS to obtain the importance function $\boldsymbol{\psi}$.

The sensitivity of head with respect to the recharge boundary condition can therefore be obtained in a single MODFLOW run. While the forward problem is non-linear, the adjoint problem is linear with passive boundary conditions. That is, there is no loading except at the node of interest. The method was implemented in MODFLOW-96 (McDonald, 1996), with only minimal additions to the existing code.

4.4 Model Application

As discussed previously, the recharge boundary condition for the groundwater model was estimated using the physically based recharge methodology, which considered detailed information about the land use and soils in the study area. The land use and soil based recharge rates were then averaged over the model grid to obtain the recharge boundary condition for the groundwater flow model.

Using the same analogy, the sensitivities in [19] can be related back to the original land use and soil based recharge rates through the chain rule as

$$\frac{\partial M}{\partial \mathbf{R}^T} = \frac{\partial M}{\partial \mathbf{X}^T}\frac{\partial \mathbf{X}}{\partial \mathbf{R}^T} = -\sum_{i=1}^{n} \tilde{\psi}_i \Delta r_i \Delta c_i \hat{a}_i \quad [20]$$

where R are the land use and soil based recharge rates, n is the number of grid blocks intersecting each unique land use and soil area, and $\hat{a}_i$ is the proportion of the area within each of the intersected grid blocks i. Equation [20] therefore allows the assessment of the impact of recharge on the groundwater flow system independent of the groundwater model discretization.

The land use and soil based recharge rates (a total of 7357 unique combinations) were assumed to be log-normally distributed, while the coefficient of variation (COV) was used to reflect uncertainty in the estimates. The same COV was assumed for all recharge rates in each simulation.

The objective of the reliability analysis was to find the distribution of recharge (with a specified level of uncertainty) that would cause the head in the well to be less than or equal to a specified target level. All simulations were run until the limit-state equation, i.e. the head difference in the well was less than 0.001 m. To simplify the analysis, all simulations were done under steady-state conditions. The steady-state pumping rate at Well 22 was equal to 2715 m^3/day. The algorithm was computationally very efficient as convergence was generally obtained in only a few iterations. The mean point in the standard normal space was used as the starting point for all simulations.

4.5 Results and Discussion

Figure 19 shows the importance or impulse function $\boldsymbol{\psi}$ obtained from the backward problem. The value of the function decreases exponentially with distance from the well as a result of the unit injection of water into the system at the well.

A typical result of the reliability analysis is shown in Figure 20. In this case, the target head was assumed to be 0.6 m below the mean value, with a COV of 0.3 for the recharge rates. The plot illustrates the difference in recharge between the mean condition (i.e. average annual recharge distribution) and the distribution of recharge that resulted in failure (i.e. the most likely realization of recharge that resulted in the head being equal to 0.6 m below the mean value at Well 22).

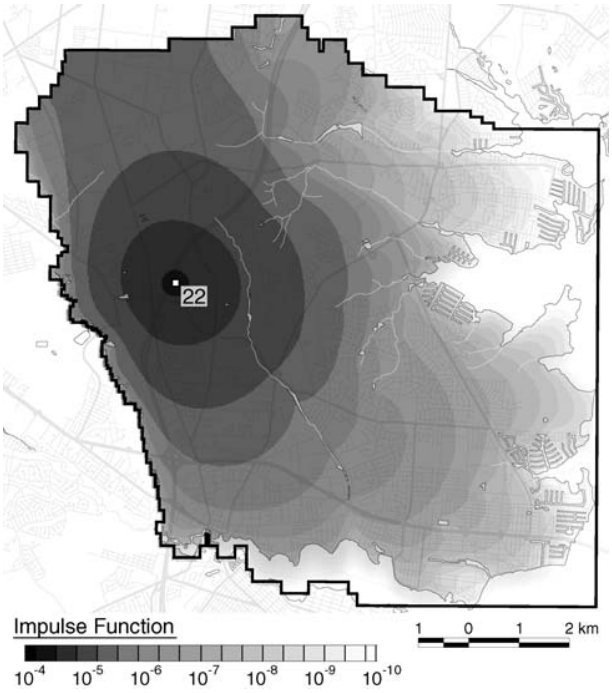

Figure 19. Importance function for groundwater flow for Well 22

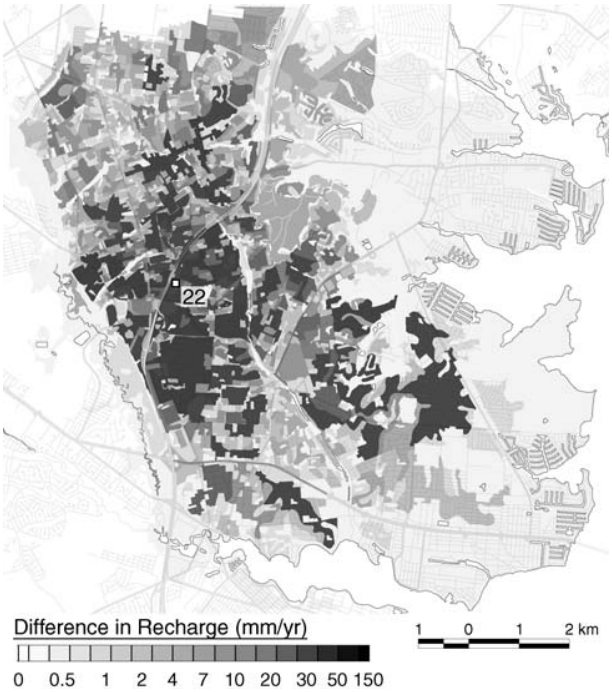

Figure 20. Difference in recharge for Well 22 resulting from a recharge COV of 0.3.

It is evident from Figure 20 that areas with higher initial recharge rates have a higher influence on the head at the well, while areas such as highways with low initial recharge rates have a smaller impact. The estimated probability of failure, i.e. the probability that the head is

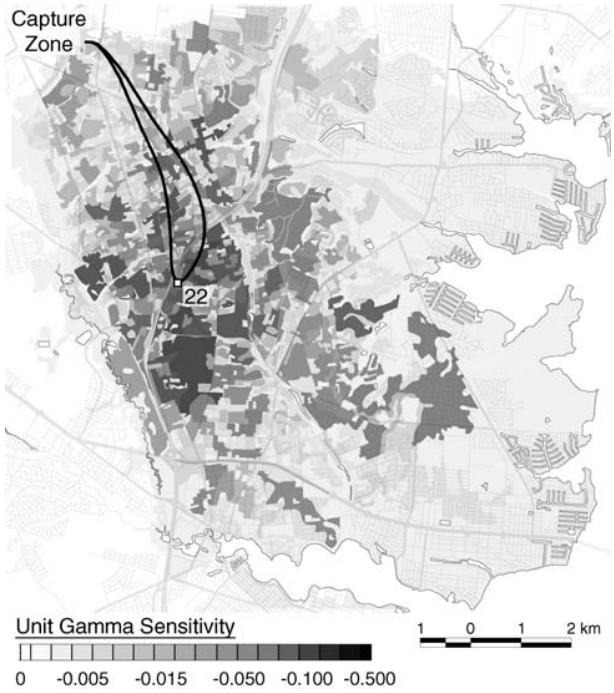

Figure 21. Unit gamma sensitivity for Well 22

greater than or equal to 0.6 m below the mean condition, was equal to 0.0017.

The relative importance of each of the input parameters, i.e. individual recharge rates, on the probabilistic outcome are shown by the unit gamma sensitivities in Figure 21. The steady-state capture zone for Well 22 is also included in Figure 21. As indicated by [9], the unit gamma sensitivity is scaled by the standard deviations and measures the sensitivity of the reliability index with respect to equally likely changes in the random variables, i.e. the recharge rates. The negative signs indicate an inverse relationship, that is, increasing the recharge rates will result in a decrease in the probability of failure. In other words, increasing recharge will increase the reliability of the head at the well.

The most important feature of Figure 21 is that it identifies areas that have the most impact on the probability of failure (or reliability) at the well. Darker areas contribute more to the probability of failure, or the probability that the head at the well will decrease by 0.6 m. It is evident that areas that are quite distant from the pumping well (and also down-gradient and outside the steady-state well capture zone) can have a significant impact on the head at the well. Therefore, Figure 21 demonstrates how land use planning and management decisions based purely on the water quality criteria (as dictated by the wellhead protection programs) may not protect the head, and hence, production at a well.

The probability of failure increases with increased uncertainty in the estimated recharge distribution. For example, for COV of 0.5 there is an 83% probability that the head at the well is less than or equal to 0.5 m below

the mean level (i.e. the drawdown at the well exceeds 0.5 m), while the probability is 38% for COV of 0.4 and 3% for COV of 0.3. Increasing the confidence in the estimated recharge distribution will therefore decrease the probability of failure (or increase the reliability) of the simulated head at the well.

5. CONCLUSIONS

Both the transient forward average water particle tracking method and the backward advective dispersive transport method demonstrate the effect of transients upon capture zones. It is not uncommon that average water particles in one well's capture zone, would migrate to a different well once the first well is taken out of service. It is also evident that an average water particle departing from the same location, but at different times, can ultimately be captured by various wells, as can be seen by the likelihood plots for particles departing from the vicinity of Reich Farm.

The reliability analysis method was integrated with MODFLOW to study the influence of the recharge boundary condition on the groundwater flow system. The spatially varying mean recharge distribution was derived from detailed soil and land use information, while the coefficient of variation was used to reflect uncertainty in the estimates. The performance function was formulated in terms of the head or flow rate at a pumping well.

The heavy computational burden of calculating the gradient sensitivity vector in the reliability analysis was overcome efficiently by implementing the adjoint method in MODFLOW. Consequently, the sensitivity of the performance function to recharge in all the grid blocks in the model could be computed in a single MODFLOW run with only minimal changes to the original MODFLOW code. The influence of the original physically based recharge distribution on the performance function was furthermore obtained using the grid block marginal sensitivities. This allowed the assessment of the impact of recharge on the groundwater flow system independent of the groundwater model discretization.

It was concluded that the sensitivity of head at the well is not only dependent on distance, but also on the size of the finite difference grid blocks and hence total recharge for the grid block. While areas with higher initial recharge rates had a higher influence on the simulated head at the well, distant land use areas that were outside the traditional well capture zone also had a significant impact on the head at the well, as identified by the normalized gamma sensitivity coefficient. Therefore, land use planning and management decisions based purely on the water quality criteria (as dictated by the traditional wellhead protection programs) may not necessarily protect the head, and hence, production at a well. Although the methodology was subject to some assumptions and limitations, it clearly demonstrated the potential of using the reliability method in probabilistic groundwater flow modelling.

References

Hasofer, A.M., and N. Lind. 1974. "An exact and invariant first-order reliability format". Journal of Engineering Mechanics, 100(1), pp. 111-121.

Jang, Y.-S., N. Sitar, and A. Der Kiureghian. 1994. "Reliability analysis of contaminant transport in saturated porous media". Water Resources Research, 30(8), pp. 2435-2448.

Jyrkama, M.I., J.F. Sykes, S.D. Normani. 2002. "Recharge Estimation for Transient Ground Water Modeling". Groundwater, 40(6), pp. 638-648.

McDonald, M.D., and A.W. Harbaugh. 1996. "A Modular Three-Dimensional Finite Difference Groundwater Flow Model". United States Geological Survey.

Rackwitz, R., and B. Fiessler. 1978. "Structural reliability under combined load sequences". Computers and Structures, 9, pp. 489-494.

Sharma, M.L. (ed.) 1989. "Groundwater Recharge". Proceedings of the Symposium on Groundwater Recharge, Mandurah, Australia, 6-9 July 1987, A.A. Balkema, Rotterdam.

Sitar, N., J.D. Cawlfield, and A. Der Kiureghian. 1987. "First-Order Reliability Approach to Stochastic Analysis of Subsurface Flow and Contaminant Transport". Water Resources Research, 23(5), 794-804.

Sykes, J.F., J.L. Wilson, and R.W. Andrews. 1985. "Sensitivity analysis for steady state groundwater flow using adjoint operators". Water Resources Research, 21(3), 359-371.

Zapecza, Otto S., 1989. "Hydrogeologic Framework of the New Jersey Coastal Plain – Regional Aquifer System Analysis - Northern Atlantic Coastal Plain", U.S. Geological Survey Professional Paper 1404-B